Study of Partial Oxidation of Methane by Ni/Al₂O₃ Catalyst: Effect of Support Oxides of Mg, Mo, Ti and Y as Promoters

Ahmed A. Ibrahim [1,*] , **Wasim U. Khan** [1], **Fahad Al-Mubaddel** [1,2], **Ahmed S. Al-Fatesh** [1,*] , **Samsudeen O. Kasim** [1] , **Sofiu L. Mahmud** [1], **Ateyah A. Al-Zahrani** [1], **M. Rafiq H. Siddiqui** [3] and **Anis H. Fakeeha** [1]

[1]   Chemical Engineering Department, College of Engineering, P.O. Box 800, Riyadh 11421, Saudi Arabia;
      wasimkhan@gmail.com (W.U.K.); falmubaddel@ksu.edu.sa (F.A.-M.); sofkolajide2@gmail.com (S.O.K.);
      mahmudsofiu@gmail.com (S.L.M.); aazz@ksu.edu.sa (A.A.A.-Z.); anishf@ksu.edu.sa (A.H.F.)
[2]   King Abdullah City for Atomic & Renewable Energy: Energy Research & Innovation Center (ERIC) in
      Riyadh, Riyadh 11451, Saudi Arabia
[3]   Chemistry Department, King Saud University, P.O. Box 2455, Riyadh 11451, Saudi Arabia; rafiqs@ksu.edu.sa
*   Correspondence: aidid@ksu.edu.sa (A.A.I.); aalfatesh@ksu.edu.sa (A.S.A.-F.)

Abstract: Catalysts of 10% Ni, supported on promoted alumina, were used to accomplish the partial oxidation of methane. The alumina support was doped with oxides of Mo, Mg, Ti and Y. An incipient wetness impregnation technique was used to synthesize the catalysts. The physicochemical properties of the catalysts were described by XRD, H_2-TPR (temperature programmed reduction), BET, TGA, CO_2-TPD (temperature-programmed desorption) and Raman. The characterization results denoted that Ni has a strong interaction with the support. The TGA investigation of spent catalysts displayed the anticoking enhancement of the promoters. The impact of the support promoters on the catalyst stability, methane conversion and H_2 yield was inspected. Stability tests were done for 460 min. The H_2 yields were 76 and 60% and the CH_4 conversions were 67 and 92%, respectively, over Ni/Al₂O₃+Mg, when the reaction temperatures were 550 and 650 °C, respectively. The performance of the present work was compared to relevant findings in the literature.

Keywords: Al₂O₃; CH_4; partial oxidation; support promoters; synthesis gas; Ni catalyst

1. Introduction

The depletion of fossil fuel resources despite their growing demand and utilization has posed prominent concerns. Thus, researchers focused on the transformation of natural gases into invaluable chemical compounds [1,2]. Natural gas, which is mainly composed of CH_4 is often converted into useful products such as synthesis gas (H_2 and CO), which is versatile and beneficial in producing chemicals like methanol and ethane [3–5]. At present, many technologies exist for CH_4 reforming to generating synthesis gas. Steam reforming which is used on a large scale has H_2/CO of 3, while dry reforming which has attracted the attention of many investigators due to the environmental aspects, generates synthesis gas of H_2/CO of 1 [6–10]. Currently, partial oxidation of CH_4 (POM) is seen to be a substitute method for both steam and dry reforming in synthesis gas production. POM draws the consideration due to its benefits, such as mild exothermicity, high efficiency, and giving an appropriate H_2/CO ratio of 2 and, therefore, it can prevent several disadvantages of the endothermic reaction of steam or dry reforming of CH_4 [11–13]. Catalytic methods used in the production of synthesis gas via POM can be categorized into two main metal-based groups: transition catalysts and noble catalysts [14–18]. Noble metals such as Rh, Pt and Pd are costly which render their utilization an

economic issue, even though they are active and stable for the conversion of CH_4 [19]. It is obligatory to seek appropriate substitutes which are not expensive. The transition metals like Ni, Co and Fe are the feasible choices [20]. Ni catalysts have been broadly examined due to their cheap cost and comparatively higher activity in the POM. Nevertheless, Ni-based catalysts are hampered by rapid catalyst deactivation as a result of Ni sintering [21,22] and phase changing of the supported constituents during the reaction [23]. Recently, researchers have been engaged in exploring the possibilities of optimizing Ni-based catalysts which are branded for a cheap price and high activity. The optimization technique stipulates wide dispersion of metal particles in the catalyst by selecting proper support, which limits the sintering and aggregation of the active species [22]. It is evident that the performance of Ni catalysts relies on the support [24]. Moreover, to alter metal-supported interactions, several metal oxides with high surface area and thermal stability like Al_2O_3, MgO, TiO_2 and the like have been used to minimize deactivation [25]. The mixture of Al_2O_3 and MgO form spinel of $MgAl_2O_4$ which is characterized by high resistance to coke depositions through stronger interactions with nickel nanoparticles [26]. Furthermore, the MgO component has the same crystal structure as NiO. The NiO–MgO solid solution develops a strong ionic bond between metal phase and support that reduces coke formation [27]. Recent studies of Ni-based catalysts have been performed with alumina or silica supports [28]. Zhang et al. reported that Ni supported on aluminate displays better activity and stability than on other supports [29]. Jalali et al. investigated Ni-based nanocatalysts employing various kinds of support for the production of synthesis gas through combined dry and partial reforming of CH_4 [30]. The results of activity and stability performance denoted that the Ni catalyst supported on $NiAl_2O_4$ displayed a 2% rise in activity. In the study of Alvarez-Galvan et al., the influence of support type on POM to produce synthesis gas, using wet impregnation and solid-state reaction, was presented [31]. They found alumina support gave the best performance on both preparation methods. This was credited to the high presence of Ni on the alumina surface. Diaz and Assaf studied CO_2 reforming of CH_4 by promoting the alumina support with basic metal oxide and they found that the modified support diminished the carbon deposition and retarded the deactivation [32]. Claude et al. reported the improvement of the catalytic performances and lifespan of Ni/γ-Al_2O_3 catalysts doped with species like Mo for steam reforming of toluene [33]. Mo-doped Ni/γ-Al_2O_3 catalysts exhibited the high reforming activity of toluene and low quantities of carbon formation. The highest performance was registered at 650 °C. Zhong-yu et al. [34] investigated the impact of Cu and Mo components of γ-Al_2O_3-supported Ni catalysts on hydro deoxygenation of fatty acid methyl esters. The promoters demonstrated better catalytic competence than Ni/γ-Al_2O_3 catalysts. Mo in the catalysts had two states: Mo^{4+} and Mo^{6+}. Shah et al. examined the dry reforming of CH_4 employing an Ni-based catalyst and TiO_2-Al_2O_3 combined as support [35]. The results displayed that doping of Al_2O_3 with TiO_2 boosted the catalytic activity and stability. Li-jun et al. [36] studied C_3H_8 catalytic combustion employing Ag-Mn/γ-Al_2O_3-TiO_2 catalysts. Results showed that composite support promoted the dispersion of Ag and Mn elements on the surface of the catalyst and created a strong interaction between the active metals, in order to augment the relative amount of reactive O_2 species and enhance the reducibility of catalysts, which upgraded the catalytic activity of C_3H_8 combustion. Zhang et al. [37] tested the catalytic performance of NiMo support on Al_2O_3-TiO_2 for HDS of 4, 6-dimethyldibenzothiophene. The composite support evidenced great specific surface area, high thermal stability and slight pore size distributions. The addition of TiO_2 could affect the interactions between metal and support, therefore, improved the reduction of active metals. The catalytic results revealed that the conversion over the catalysts slowly increased as the Ti/Al molar ratio increased to 0.4. Abdollahifar et al. used an Ni-Co/Al_2O_3–MgO nanocatalyst for H_2 production by dry reforming of CH_4 [38]. The nanosynthesized Ni-Co/Al_2O_3–MgO displayed the suitability of the active phases in the presence of the combined support. Alibi et al. [39]; reported the benefit of using Ni and Ni-Co support on a mixture of Mg and alumina-supported catalysts with various concentrations of Mg and Al for dry reforming of methane. Their results displayed a remarkable enhancement of conversion, selectivity, and resistance to carbon formation, particularly when the Mg/Al ratio was bigger than unity. These effects were due to the

improvement of active metal reduction, metal support and metal−metal interactions. Khoja et al. [40] also investigated the influence of the combined support of Mg and Alumina for the same reaction, employing a cold plasma dielectric barrier discharge reactor. They found that the addition of MgO to Ni/Al$_2$O$_3$ helped to increase the basicity of the support and enhanced the interaction of Ni and Al$_2$O$_3$, which affected the reducibility and stability. Jung et al. [41] studied steam reforming of CH$_4$, employing a series of Ni-MgO-Al$_2$O$_3$ catalysts for fuel cells. They tested MgO loadings of 3 to 15 wt%. Their results displayed the highest conversion of methane and resistance against K poisoning when a 10 wt.% MgO support was used. The superb performance of reforming is related to the large interaction of Ni and alumina support when MgO is coprecipitated with the Ni-Al$_2$O$_3$. The improved interaction of the Ni with MgO−Al$_2$O$_3$ support protected the Ni against K poisoning. Özdemir and Öksüzömer examined the performance of Al$_2$O$_3$, MgO and MgAl$_2$O$_4$ supports on 10% Ni catalyst in the partial oxidation of methane [41,42]. The catalyst supported by the combination of Mg and Al showed the highest activity and selectivity. High conversion of CH$_4$ and constant H$_2$/CO for 20 h was reported. Yttria (Y$_2$O$_3$) is extensively used as a sintering additive to strengthen Al$_2$O$_3$ [43]. Y$_2$O$_3$ is reported as an effective additive in preparing ceramics to increase mechanical properties by minimizing interfacial reactions, increasing oxidation resistance, consolidating grain boundaries and regulating grain size [44]. Y$_2$O$_3$ has been reported to form NiYO$_3$ compound with Ni, causing the alteration of coke and coke location in the autothermal reforming of methane [45]. Hongbo et al. [46] performed steam reforming of ethanol at a low temperature for hydrogen production using Ni/Y$_2$O$_3$-Al$_2$O$_3$ catalysts. They used Y$_2$O$_3$- Al$_2$O$_3$ with different mole ratios. The result of composite support had a suitable synergistic effect between the active constituent and support, and NiO could be reduced easily and hence the composite support catalysts displayed high activity for ethanol steam reforming. Santos et al. [45] studied the influence of yttrium oxide addition to Ni/α-Al$_2$O$_3$ catalysts in autothermal reforming of CH$_4$. The Y$_2$O$_3$-Al$_2$O$_3$ supported catalysts offered high performance. The upgraded stability of catalysts resulted from the decrease of coke on the surface of Ni. A similar reaction process was performed by Sun et al. [47] who investigated the impacts of Y$_2$O$_3$-doping to Ni/γ-Al$_2$O$_3$ catalysts during the autothermal reforming of CH$_4$ to H$_2$ and CO. The results of different loadings of Y$_2$O$_3$ (5%, 8%, 10%) showed substantial enhancement in performance. The Ni supported on Y$_2$O$_3$+γ-Al$_2$O$_3$ had greater NiO reducibility, minor Ni particle size, wider Ni dispersion than those of the pristine Ni/γ-Al$_2$O$_3$ catalysts. Therefore, the mixture support repressed the sintering of Ni, transformed the type of coke and reduced the content of coke on the catalysts.

The purpose of this study is to work out the best textural promoter of Al$_2$O$_3$ support on Ni catalyst to achieve high activity and stability, while minimizing the carbon formation during the POM process. The influence of promoters like oxides of Y, Ti, Mg, and Mo on the activity, stability, and coke formation of promoted γ-Al$_2$O$_3$ supported on Ni catalysts were surveyed. Numerous characterization techniques were used to better understand the catalytic performance.

2. Results and Discussion

The textural properties of Ni-Al-x (x = 0, Mo, Ti, Y, and Mg) were evaluated using the N$_2$ adsorption−desorption isotherms. Supplementary Figure S1 displays the N$_2$ adsorption−desorption isotherms of the fresh catalysts calcined at 650 °C. According to the IUPAC classification, the catalysts display a type IV isotherm with a hysteresis loop of the H3-type, resulting from capillary condensation and evaporation at elevated P/P$_0$ [48]. The rise in the amount of N$_2$ adsorbed at high P/P$_0$ in the isotherm curves is due to the phenomenon of capillary condensation within the sample pores. The sorption isotherms of all the catalysts are alike, designating that there is almost no change in the pore structure of the support when modified with the metal oxides. Table 1 depicts the BET surface area, average pore diameter, and pore volume.

Table 1. Textural properties of Ni-Al-x (x = 0, Mo, Ti, Y, and Mg) catalysts.

Samples	S_{BET} (m^2/g)	V_P (cm^3/g)	d_P (nm)
Ni-Al	173.1	0.613	12.20
Ni-Al-Mo	161.0	0.558	12.42
Ni-Al-Ti	165.0	0.586	12.71
Ni-Al-Mg	172.8	0.603	12.46
Ni-Al-Y	176.3	0.630	12.35

Figure 1 displays the XRD profiles of fresh Ni-Al-x (x = 0, Mo, Ti, Y, and Mg) catalysts. The samples showed the XRD peaks of γ-Al$_2$O$_3$ at 2θ = 37.2, 45.8 and 66.4° (JCPDS 86-1410). The peaks for NiO overlapped those of γ-Al$_2$O$_3$ and appeared at 2θ = 37.2, 45.8 and 66.4° (JCPDS 47-1049), with the reflections of 111, 200, 220, respectively, suggesting that these Ni-containing phases were highly dispersed on the surface of the supports. The modification of the alumina support with Mo did not have any influence on the characteristic peaks depicting the uniform scattering Mo in the matrix of Ni-Al. On the other hand, the addition of 10% of Mg, Ti and Y oxides maintained the characteristic peaks of the Ni/γ-Al$_2$O$_3$. However, some additional peaks appeared related to the particular metal oxide. For instance, the characteristic peaks of MgO occurred at 2θ = 43.3° and 63.1°, the peaks of TiO$_2$ appeared at 2θ = 25.1° and 54.3°, while Y$_2$O$_3$ appeared at 2θ = 29.0°, 48.4° and 58.1° (JCPDS 083-0927).
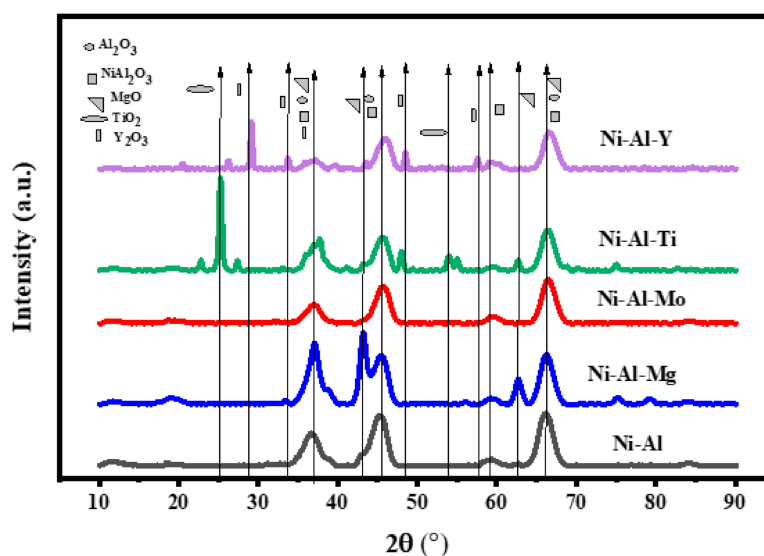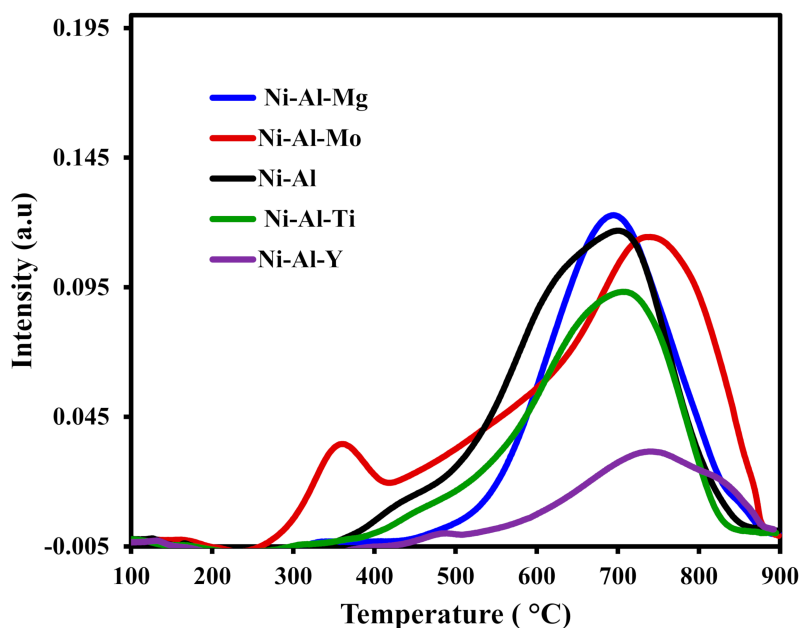

Figure 1. The XRD profiles of Ni-Al-x (x = 0, Mo, Ti, Y, and Mg) catalysts.

Figure 2 shows the H$_2$-TPR (temperature programmed reduction) curves of the fresh catalysts: Ni-Al-x (x = 0, Mo, Ti, Y, and Mg). No clear reduction peak was detected in the range of 200−400 °C for all the catalysts except the catalyst supported on Mo-modified alumina, signifying the nonappearance of dissociated or free NiO in the prepared catalysts. However, for the case of the Mo-modified catalyst, there was an additional reduction peak at around 300−440 °C, which denoted the weak interaction of dissociated or free NiO with Al$_2$O$_3$-Mo support. Virtually all the catalysts were characterized by two peaks. The peak that appeared before 500 °C, with varying intensities, could be ascribed to moderate interaction between NiO and the Al$_2$O$_3$. The second broad reduction peak appeared within the range of 700–880 °C. This was assigned to NiAl$_2$O$_4$, which resulted from the strong interaction of Al$_2$O$_3$ with NiO [49]. The addition of promoters to the support did not enhance the reducibility of the catalysts according to the TPR profiles.

Figure 2. Temperature programmed reduction (TPR) profiles of the fresh Ni-Al-x (x = 0, Mo, Ti, Y, and Mg) catalysts.

Catalytic Performance

The activities of all five catalysts: Ni-Al-x (x= Mo, Ti, Y, and Mg), and Ni-Al were investigated in partial oxidation of CH_4 over the reduced catalysts under the same reaction conditions at 550 and 650 °C for approximately 8 h. The outcomes of the experiments are shown in Figure 3. Figure 3A depicts the CH_4 conversion as a function of time on stream (TOS). On the one hand, no substantial reduction in conversion was identified in the activity of Ni-Al-Ti catalyst, which suggests the stability of the catalyst. The catalyst had 60% initial CH_4 conversion and nearly maintained that value. On the other hand, Ni-Al-Mg, Ni-A-Mo and Ni-Al$_2$O$_3$ catalysts gave the highest initial CH_4 conversions of about 68.0, 67.7, 67.7% with reductions of 5.7, 8.1, 8.1%, respectively, over the time on stream. Ni-Al-Y catalyst gave the lowest initial conversion of 50% and a 6.6% reduction. Figure 3B displays the H_2 yield versus time on stream. Ni-Al-Mg catalyst gave the highest initial H_2 yield of about 60%, while the Ni-Al-Y catalyst presented the lowest initial H_2 yield of about 39.2%. Figure 3C shows the CH_4 conversion versus time on stream setting the temperature at 650 °C. Higher CH_4 conversions were observed as a result of the increase in the reaction temperature. No sizable reduction in conversion was observed for all catalysts, suggesting the existence of good stability in their TOS. Ni-Al-Mg catalyst gave the highest CH_4 conversion of about 92%, whereas the Ni-Al-Y catalyst provided the least conversion of about 88%. Figure 3D shows the H_2 yield profiles against TOS. The stability of the catalysts was quite good since the drop in the yield of H_2 was less than 3% in all cases over the TOS. The Ni-Al-Mg catalyst gave the greatest H_2 yield of about 76% while the Ni-Al-Y catalyst had the least H_2 yield of about 71%. The promoting alumina with Mg, Mo and Ti enhanced the performance of the catalysts, while the Y promoter lowered the performance. These characteristics of promoters were obvious at lower reaction temperatures. Supplementary Figures S2 and S3 display the CO yield versus time on stream at 550 and 650 °C reaction temperatures, respectively.

Table 2 compares the efficiency of the catalysts used in this work to the partial oxidation results obtained by other investigators. It is evident that the work performed in this manuscript is worth sharing with other investigators in the field.
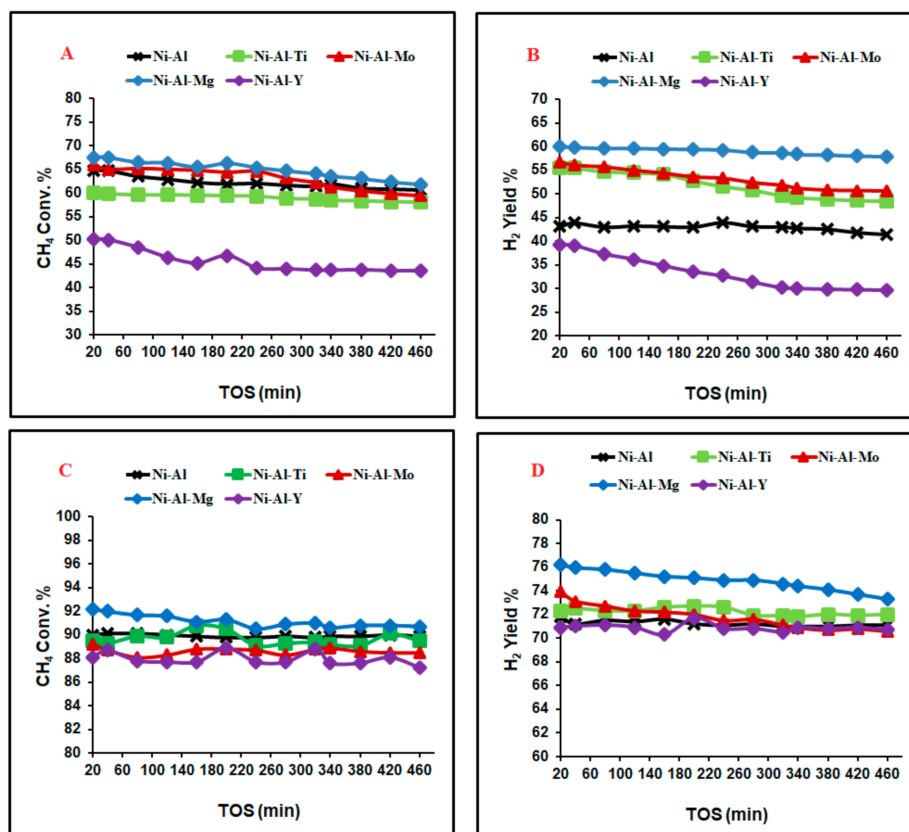
Figure 3. (**A**) CH_4 conversions reaction temperature 550 °C; (**B**) hydrogen yield reaction temperature 550 °C; (**C**) CH_4 conversions reaction temperature 650 °C; (**D**) hydrogen yield reaction temperature 650 °C; as a function of time-on-stream over the Ni catalysts. (mass of catalyst, 0.1 g; $CH_4:O_2$ = 2:1, 1 atom; and flow rate, 32.5 mL/min.).

Table 2. Assessment of CH_4 partial oxidation.

Sample	Mass mg	Methane/Oxygen	Space Velocity (ml/min)	Test Temperature (°C)	Methane Conversion (%)	Reference
La $Ni_{0.5}Nb_{0.5}O_3$	30	2:1	100	750	64	[50]
10% Ni/NiAl$_2$O$_4$- MgAl$_2$O$_4$	100	CH_4: CO_2: O_2 2:1:0.5	140	700	70	[29]
$Ni_{0.05}Cu_{0.05}Mg_{0.9}/Al_{0.5}$	200	2:1	60	750	88	[1]
5%Ni/Al$_2$O$_3$	100	2:1	40.6	750	85	[31]
10%Ni+0.1%Rh/Al$_2$O$_3$	100	2:1	40.6	750	88	[31]
10%Ni+1%Re/γ-Al$_2$O$_3$	100	2:1	100	600	66.2	[51]
10%Ni/Al$_2$O$_3$+Mg	100	2:1	32.5	650	92	This work

The strength type of basic sites can be categorized by the temperature of the related desorption peaks: the ranges of 50–200 °C, 200–400 °C, 400–650 °C, above 650 °C, are commonly ascribed to the weak, intermediate, strong and very strong, respectively. Figure 4 depicts the CO_2 temperature-programmed desorption, which evaluates the basicity of Ni-based catalysts on the basic sites at different temperatures.

For the Ni-Al catalyst, there were peaks at 72, 245, and at 772 °C, attributable to the weak, intermediate, and very strong basic sites, respectively. For the Ni-Al-Mo catalyst, a similar pattern of peaks was observed at 102, 245 and 775 °C, indicating that the addition of Mo did not alter the basicity. For the Ni-Al-Mg catalyst, there were three peaks. The first two peaks were similar to the unmodified alumina supported catalyst; however, the third peak appeared at 522 °C, denoting strong but not very strong basicity. For the Ni-Al-Ti catalyst, there were four peaks at 73, 124, 248 and 510 °C. Two peaks were in the weak basicity region, while the remaining two peaks were similar to that of

Mg-modified support, showing intermediate and strong basicity. However, when Y was promoted with the alumina, six peaks were observed in its profile. Two of them were in the weak basicity region, where a peak was observed at 77 °C with a shoulder desorption peak of low intensity at 133 °C. Another two peaks were in the intermediate basic region, at 244 and 340 °C. The remaining two peaks appeared at 515 and 703 °C and described as strong and very strong peaks. The Y-modified supported catalyst exhibited relatively higher intensity and wider CO_2 desorption area peaks, suggesting more basicity than unmodified alumina support.
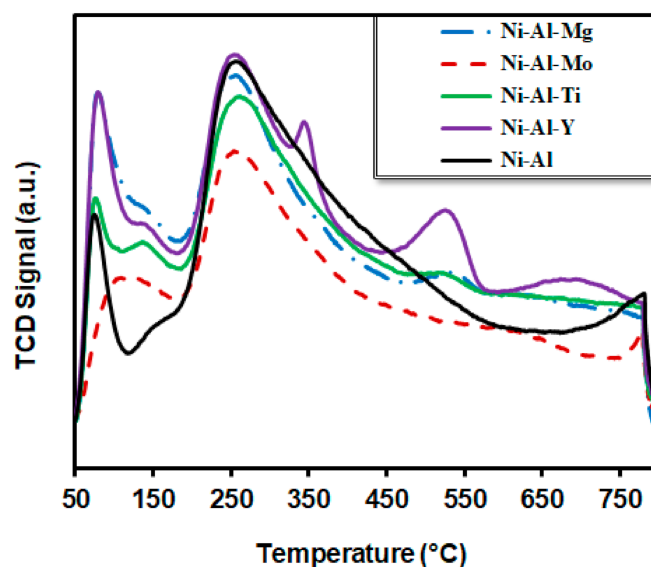
Figure 4. Represents the CO_2-temperature-programmed desorption (TPD) profiles of the Ni-Al-x (x = 0, Mo, Ti, Y, and Mg) catalysts.

Carbon deposition causes deactivation of the catalyst. TGA technique was employed to investigate the amount of carbon deposits on the used catalysts. The TGA analysis of the spent catalysts tested at 550 °C reaction temperature is given in Figure 5. The quantity of carbon formed on the catalysts was in the range of 1−6 wt.% with the unmodified support having the highest amount and the Mo-modified support having the least amount of carbon deposits. From the TGA profile of each of the catalysts, there was an increase in the weight from 400 to 500 °C. This could be attributed to the oxidization of Ni to NiO in the air atmosphere. The TGA analysis of the spent catalysts studied at 650 °C reaction temperature is given in Figure 6. The quantity of carbon formed on the catalysts was in the range of 4−6.8 wt.% and different for each, while the drop in CH_4 conversion of the catalysts was 9.3−12.8% in Figure 3, which was related to the experiment time of approximately 8 h. Mo-modified support catalyst had the least amount of carbon deposits while Y-modified support had the highest. For the TGA profile of Mo-modified support catalyst, there was an increase in weight from 430 to 540 °C, which could be attributed to the oxidization of Ni to NiO in the air atmosphere.

Supplementary Figure S4 illustrates the Raman spectra of spent Ni-Al-y (y = 0, Mo, Ti, Y, and Mg) catalysts attained for 7 h using a 550 °C reaction temperature. Two similar intensity peaks appeared at 1473 cm^{-1} and 1535 cm^{-1}, corresponding to the D band, ascribed to sp3 hybridized amorphous carbon, and G band, indicated by the occurrence of graphitized carbon, respectively. The D band and G band are characteristic bands of regular-structured carbon that occur on the surface of Ni-Al-y (y = 0, Mo, Ti, Y, and Mg) in the course of the partial reforming reaction. The peak areas ratio of the D and G (I_D/I_G) bands is employed to evaluate the graphitic degree and the amount of defects in spent catalysts, a low I_D/I_G ratio denoting higher structural perfection of the spent catalysts. The ratio of I_D/I_G as 1.03, 1.04, 1.10, 1.12 and 1.17 was computed respectively, for Ni-Al-Ti, Ni-Al-Ti, Ni-Al, Ni-Al-Y, Ni-Al-Mo and Ni-Al-Mg catalysts. This displays that the degree of graphitization decreased for spent Ni-Al-Mg, which is consistent with the best catalytic performance of CH_4 conversion and hydrogen

yield. The Raman analysis also depicted that the Ni-Al catalyst possessed the highest peak and highest carbon deposition, while Ni-Al-Mo catalyst had the least, in conformity with the TGA analysis of Figure 5. Supplementary Figure S5 shows the Raman spectra of spent Ni-Al-y (y = 0, Mo, Ti, Y, and Mg) catalysts obtained for 7 h using a 650 °C reaction temperature. Two analogous intensity peaks emerged around 1469 cm^{-1} and 1532 cm^{-1}, corresponding to the D band, allocated to sp3 hybridized amorphous carbon, and G band, denoted by the existence of graphitized carbon, respectively. The intensities of the peaks of Ni-Al and Ni-Al-Y were higher than those of the other catalysts. The ratio of I_D/I_G was computed to 0.89, 1.02, 1.03, 1.08, 1.12 and 1.24 for Ni-Al-Y, Ni-Al-Ti, Ni-Al-Mo, Ni-Al and Ni-Al-Mg catalysts, respectively.
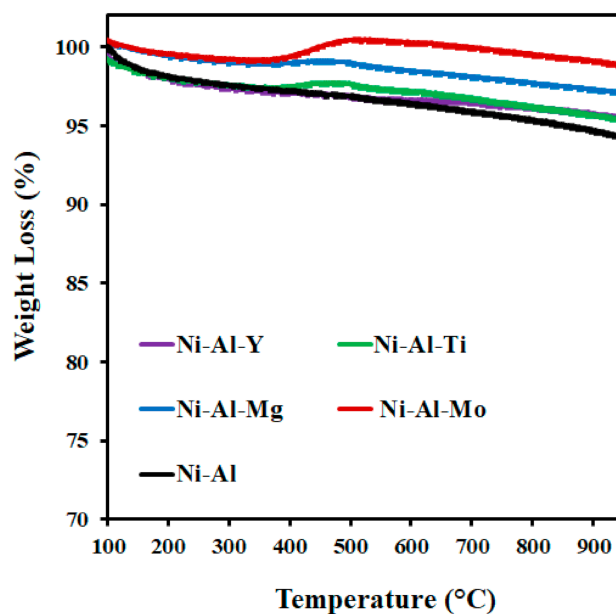

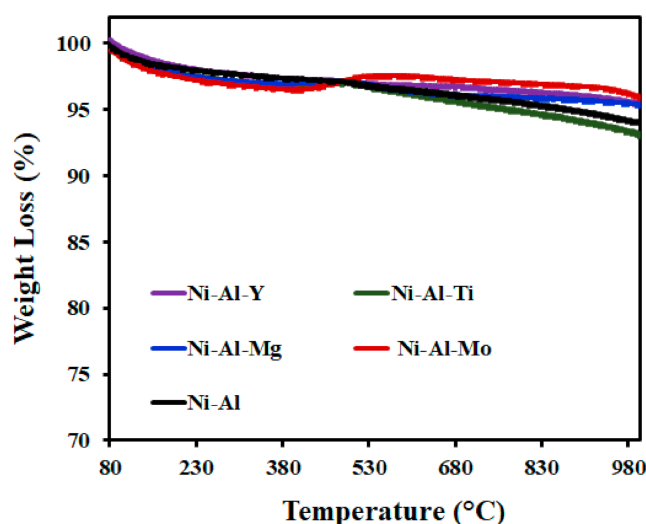**Figure 5.** TGA of the spent catalysts tested at 550 °C.

Figure 6. TGA of the spent catalysts studied at 650 °C.

3. Experimental

3.1. Catalyst Development

A wet impregnation procedure was used to obtain the catalysts for the catalyst of 10% Ni supported on 10%X + 80% Al_2O_3 (X= Mo, Ti, Y, and Mg). Ninety percent of the support was impregnated with

10% Ni obtained from hydrated nickel nitrate $Ni(NO_3)_2 \times 6H_2O$. The nickel nitrate was first dissolved in 30 mL deionized water followed by the support after having a uniform solution. The catalyst was calcined at 650 °C after drying at 120 °C in a furnace. The prepared catalysts were designated as shown in Table 3.

Table 3. Designations of the catalysts used in this analysis.

Sample Name	Sample Formation
Ni-Al	10%Ni/90% Al_2O_3
Ni-Al-Mo	10%Ni/10%Mo+80% Al_2O_3
Ni-Al-Mg	10%Ni/10%Mg+80% Al_2O_3
Ni-Al-Ti	10%Ni/10%Ti+80%Al_2O_3
Ni-Al-Y	10%Ni/10%Y+80%Al_2O_3

3.2. Catalytic Reaction

A portion of 100 mg of catalyst was used in the partial oxidation of CH_4 operated atmospherically in a 9.1 mm diameter and 30 cm long tube reactor. PID Eng & Tech Micro provided the reactor. A thermocouple was applied to measure the reaction temperature. The feed gas compositions (methane/oxygen/nitrogen) were in the volume ratio of 3/1.5/2, with a total flow rate of 32.5 mL/min. Reaction temperatures of 550 and 650 °C were used during the experiments. A gas chromatographer (GC-2014 SHIMADZU), connected with a TCD detector using Porapak Q and Molecular Sieve 5A, was used in the analysis of the output gases. CH_4 conversion and H_2 yield were calculated using the subsequent equations:

$$CH_4 \text{ conversion} = \frac{CH_{4,in} - CH_{4,out}}{CH_{4,in}} \times 100 \tag{1}$$

$$H_2 \text{ } Yield = \frac{moles \text{ } of \text{ } H_2 \text{ } produced}{2 \times CH_{4,feed}} multiplied \text{ } by \text{ } 100 \tag{2}$$

3.3. Catalyst Description

The new and used catalysts were categorized using the following techniques:

3.3.1. Nitrogen Physical Adsorption

A Micromeritics Tristar II 3020 porosity and surface area analyzer determined the textural properties of the catalysts via adsorption–desorption isotherms using liquid nitrogen. In the test, 0.2–0.3g of the catalyst was used. At first, the sample was heated at 300 °C for three hours to drive away vapor, undesirable adsorbed gases, and organics. The specific surface area of the catalyst was determined via the BET technique and equation.

3.3.2. Temperature Programmed Reduction (TPR)

The H_2 activation of the catalyst was tested by TPR using an AutoChem-II Micromeritics. In the analysis, 0.070 g of the catalyst precursors were first heated to 150 °C and held at that temperature for 60 min in the presence of Ar at the rate of 1.8 L/h and then cooled to room temperature. Next, the sample temperature was raised to 900 °C at 10 K/min in an automatic furnace at 1 atmosphere. While heating, H_2/Ar mixture with a volume ratio of 10/90 was flowing at 2.40 L/h. The amount of H_2 consumed was determined by a thermal conductivity detector.

3.3.3. X-ray Diffractogram (XRD)

The XRD diffraction measurements were performed to detect the crystalline phases of the catalysts. The unit was from XRD Rigaku, having Kα-Cu X-ray radiation of 40 kV and 40 mA, a scanning 2θ range of 10–85° and a step of 0.02°. X'Pert high score plus software was employed to assess the data.

3.3.4. Thermo-Gravimetric Analysis (TGA)

The amount of carbon formation on the surface of the catalyst was examined by thermo-gravimetric analysis through the Shimadzu TGA analyzer. In every analysis, 0.100−0.150 g of used catalyst was heated with a ramping degree of 20 °C/min from ambient temperature to 1000 °C. The mass reduction of the sample as a result of the oxidation in the air was recorded.

3.3.5. Raman Spectroscopy

Raman spectra were performed using an NMR-4500 Laser Raman Spectrometer. A wavelength with an excitation beam of 5.32×10^3 Å was set. A lens with 20× enlargement was employed to assess the spectra. A 6 mW beam power and an exposure time of 3 min were employed. The Raman change of the spectra was calculated in the range 10^3–3×10^3 cm^{-1}. Spectra Manager Ver.2 software was used to manage the profiles.

3.3.6. CO_2-TPD

The CO_2 temperature-programmed desorption (TPD) was accomplished via Micromeritics Autochem II apparatus. Initially, 0.006 g of catalyst was activated with helium gas at 600 °C for 1 h and then the sample temperature was reduced to 50 °C. Then CO_2 was admitted and continued for 60 min. Afterward, He gas was used to flush the sample to take away any physisorbed CO_2. The peaks of desorption were noted while the temperature was varied by 10 °C/min. The CO_2 concentration in the output was recorded via a thermal conductivity detector.

4. Conclusions

This work has demonstrated the performance effect of alumina support promoters used in synthesizing Ni-based catalysts for methane partial oxidation. The oxide promoters for the support were MgO, MoO_2, TiO_2 and Y_2O_3. The promoters enhanced the catalytic activity with the exception of the Y_2O_3 oxide which inhibited the CH_4 conversion as well as the H_2 yield in comparison to the unmodified support. The order of catalytic performance with respect to promoted supports is as follows. For 550 °C reaction temperature: Ni-Al-Mg>Ni-Al-Mo>Ni-Al-Ti>Ni-Al-Y and for the reaction at 650 °C; Ni-Al-Mg>Ni-Al-Ti>Ni-Al-Mo>Ni-Al-Y. The increase of the reaction temperature from 550 to 650 °C, as expected, improved the catalytic performance and reduced the preference among the type of support promoters. The BET analysis exhibited that the un-promoted catalyst depicted a little bit lower pore volume than the promoted catalysts. From the TPR results, only Ni-A-Mo catalyst showed a peak at lower temperatures, an indication of the existence of free NiO with weak interaction between the promoter and the support. The TGA analysis performed at 550 °C reaction temperature exhibited that Ni-Al catalyst possessed the highest carbon deposit. The Raman analysis displayed amorphous carbon and graphitic carbon deposits.

Author Contributions: A.A.I., F.A.-M., A.S.A.-F. and S.O.K. synthesized the catalysts, performed all the experiments and characterization tests and wrote the manuscript; W.U.K. for writing—review and editing; S.L.M., M.R.H.S. prepared the catalyst and contributed in proofreading of the manuscript; A.A.A.-Z. for funding acquisition and resources; A.E.A., F.A.-M. and A.H.F. contributed to the analysis of the data and proofread the manuscript. All authors have read and agreed to the published version of the manuscript.

Conflicts of Interest: The authors declare no conflict of interest.

References

1. Kaddeche, D.; Djaidja, A.; Barama, A. Partial oxidation of methane on co-precipitated Ni–Mg/Al catalysts modified with copper or iron. *Int. J. Hydrog. Energy* **2017**, *42*, 15002–15009. [CrossRef]

2. Silva, C.R.B.; da Conceição, L.; Ribeiro, N.F.P.; Souza, M.M.V.M. Partial oxidation of methane over Ni–Co perovskite catalysts. *Catal. Commun.* **2011**, *12*, 665–668. [CrossRef]

3. Lunsford, J.H. Catalytic conversion of methane to more useful chemicals and fuels: A challenge for the 21st century. *Catal. Today* **2000**, *63*, 165–174. [CrossRef]

4. Pantaleo, G.; Parola, V.L.; Deganello, F.; Singha, R.K.; Bal, R.; Venezia, A.M. Ni/CeO$_2$ catalysts for methane partial oxidation: Synthesis driven structural and catalytic effects. *Appl. Catal. B Environ.* **2016**, *189*, 233–241. [CrossRef]

5. Al-Fatesh, A.S.; Atia, H.; Abu-Dahrieh, J.K.; Ibrahim, A.A.; Eckelt, R.; Armbruster, U.; Abasaeed, A.E.; Fakeeha, A.H. Hydrogen production from CH$_4$ dry reforming over Sc promoted Ni/MCM-41. *Int. J. Hydrog. Energy* **2019**, *44*, 20770–20781. [CrossRef]

6. Vahid Shahed, G.; Taherian, Z.; Khataee, A.; Meshkani, F.; Orooji, Y. Samarium-impregnated nickel catalysts over SBA-15 in steam reforming of CH$_4$ process. *J. Ind. Eng. Chem.* **2020**, *86*, 73–80. [CrossRef]

7. Kim, A.R.; Lee, H.Y.; Cho, J.M.; Choi, J.-H.; Bae, J.W. Ni/M-Al$_2$O$_3$ (M=Sm, Ce or Mg) for combined steam and CO$_2$ reforming of CH$_4$ from coke oven gas. *J. CO2 Util.* **2017**, *21*, 211–218. [CrossRef]

8. Angeli, S.D.; Monteleone, G.; Giaconia, A.; Lemonidou, A.A. State-of-the-art catalysts for CH$_4$ steam reforming at low temperature. *Int. J. Hydrog. Energy* **2014**, *39*, 1979–1997. [CrossRef]

9. Jung, Y.-S.; Yoon, W.-L.; Rhee, Y.-W.; Seo, Y.-S. The surfactant-assisted Ni–Al$_2$O$_3$ catalyst prepared by a homogeneous precipitation method for CH$_4$ steam reforming. *Int. J. Hydrog. Energy* **2012**, *37*, 9340–9350. [CrossRef]

10. Al-Fatesh, A.S.; Arafat, Y.; Ibrahim, A.A.; Atia, H.; Fakeeha, A.H.; Armbruster, U.; Abasaeed, A.E.; Frusteri, F. Evaluation of Co-Ni/Sc-SBA–15 as a novel coke resistant catalyst for syngas production via CO$_2$ reforming of methane. *Appl. Catal. A Gen.* **2018**, *567*, 102–111. [CrossRef]

11. Ma, Y.; Ma, Y.; Chen, Y.; Ma, S.; Li, Q.; Hu, X.; Wang, Z.; Buckley, C.E.; Dong, D. Highly stable nanofibrous La2NiZrO6 catalysts for fast methane partial oxidation. *Fuel* **2020**, *265*, 116861. [CrossRef]

12. Shareei, M.; Taghvaei, H.; Azimi, A.; Shahbazi, A.; Mirzaei, M. Catalytic DBD plasma reactor for low temperature partial oxidation of methane: Maximization of synthesis gas and minimization of CO$_2$. *Int. J. Hydrog. Energy* **2019**, *44*, 31873–31883. [CrossRef]

13. Shishido, T.; Sukenobu, M.; Morioka, H.; Kondo, M.; Wang, Y.; Takaki, K.; Takehira, K. Partial oxidation of methane over Ni/Mg-Al oxide catalysts prepared by solid phase crystallization method from Mg-Al hydrotalcite-like precursors. *Appl. Catal. A Gen.* **2002**, *223*, 35–42. [CrossRef]

14. Wang, H.Y.; Ruckenstein, E. Partial Oxidation of Methane to Synthesis Gas over Alkaline Earth Metal Oxide Supported Cobalt Catalysts. *J. Catal.* **2001**, *199*, 309–317. [CrossRef]

15. Khine, M.S.S.; Chen, L.; Zhang, S.; Lin, J.; Jiang, S.P. Syngas production by catalytic partial oxidation of methane over (La0.7A0.3) BO$_3$ (A = Ba, Ca, Mg, Sr, and B = Cr or Fe) perovskite oxides for portable fuel cell applications. *Int. J. Hydrog. Energy* **2013**, *38*, 13300–13308. [CrossRef]

16. López-Fonseca, R.; Jiménez-González, C.; de Rivas, B.; Gutiérrez-Ortiz, J.I. Partial oxidation of methane to syngas on bulk NiAl$_2$O$_4$ catalyst. Comparison with alumina supported nickel, platinum and rhodium catalysts. *Appl. Catal. A Gen.* **2012**, *437–438*, 53–62. [CrossRef]

17. Araújo, J.C.S.; Oton, L.F.; Oliveira, A.C.; Lang, R.; Otubo, L.; Bueno, J.M.C. On the role of size controlled Pt particles in nanostructured Pt-containing Al$_2$O$_3$ catalysts for partial oxidation of methane. *Int. J. Hydrog. Energy* **2019**, *44*, 27329–27342. [CrossRef]

18. Mateos-Pedrero, C.; Duquesne, S.; Carrazán, S.R.G.; Soria, M.A.; Ruíz, P. Influence of the products of the partial oxidation of methane (POM) on the catalytic performances of Rh/Ti-modified support catalysts. *Appl. Catal. A Gen.* **2011**, *394*, 245–256. [CrossRef]

19. Wang, F.; Li, W.-Z.; Lin, J.-D.; Chen, Z.-Q.; Wang, Y. Crucial support effect on the durability of Pt/MgAl$_2$O$_4$ for partial oxidation of methane to syngas. *Appl. Catal. B Environ.* **2018**, *231*, 292–298. [CrossRef]

20. Ding, C.; Wang, J.; Guo, S.; Ma, Z.; Li, Y.; Ma, L.; Zhang, K. Abundant hydrogen production over well dispersed nickel nanoparticles confined in mesoporous metal oxides in partial oxidation of methane. *Int. J. Hydrog. Energy* **2019**, *44*, 30171–30184. [CrossRef]

21. Wang, W.; Su, C.; Ran, R.; Park, H.J.; Kwak, C.; Shao, Z. Physically mixed LiLaNi- Al$_2$O$_3$ and copper as conductive anode catalysts in a solid oxide fuel cell for methane internal reforming and partial oxidation. *Int. J. Hydrog. Energy* **2011**, *36*, 5632–5643. [CrossRef]

22. Ding, C.; Wang, J.; Jia, Y.; Ai, G.; Liu, S.; Liu, P.; Zhang, K.; Han, Y.; Ma, X. Anti-coking of Yb-promoted Ni/Al$_2$O$_3$ catalyst in partial oxidation of methane. *Int. J. Hydrog. Energy* **2016**, *41*, 10707–10718. [CrossRef]

23. Zhang, Y.; Xiong, G.; Sheng, S.; Yang, W. Deactivation studies over NiO/γ-Al$_2$O$_3$ catalysts for partial oxidation of methane to syngas. *Catal. Today* **2000**, *63*, 517–522. [CrossRef]

24. Tsipouriari, V.A.; Zhang, Z.; Verykios, X.E. Catalytic partial oxidation of methane to synthesis gas over Ni-based catalysts: I. Catalyst performance characteristics. *J. Catal.* **1998**, *179*, 283–291. [CrossRef]

25. Fan, M.S.; Abdullah, A.Z.; Bhatia, S. Catalytic technology for carbon dioxide reforming of methane to synthesis gas. *ChemCatChem* **2009**, *1*, 192–208. [CrossRef]

26. Park, K.S.; Son, M.; Park, M.J.; Kim, D.H.; Kim, J.H.; Park, S.H.; Choi, J.H.; Bae, J.W. Adjusted interactions of nickel nanoparticles with cobalt-modified MgAl$_2$O$_4$-SiC for an enhanced catalytic stability during steam reforming of propane. *Appl. Catal. A Gen.* **2018**, *549*, 117–133. [CrossRef]

27. Min, J.E.; Lee, Y.J.; Park, H.G.; Zhang, C.; Jun, K.W. Carbon dioxide reforming of methane on Ni-MgO-Al$_2$O$_3$ catalysts prepared by sol-gel method: Effects of Mg/Al ratios. *J. Ind. Eng. Chem.* **2015**, *26*, 375–383. [CrossRef]

28. Jilei, Y.; Zengxi, L.; Huachao, D.; Yuan, L. Lanthanum Modified Ni/y-A1$_2$O$_3$ Catalysts for Partial Oxidation of Methane. *J. Rare Earths* **2006**, *24*, 302–308.

29. Zhang, R.J.; Xia, G.F.; Li, M.F.; Wu, Y.; Nie, H.; Li, D.D. Effect of support on catalytic performance of Ni-based catayst in methane dry reforming. *Ranliao Huaxue Xuebao J. Fuel Chem. Technol.* **2015**, *43*, 1359–1365. [CrossRef]

30. Jalali, R.; Rezaei, M.; Nematollahi, B.; Baghalha, M. Preparation of Ni/MeAl$_2$O$_4$-MgAl$_2$O$_4$ (Me = Fe, Co, Ni, Cu, Zn, Mg) nanocatalysts for the syngas production via combined dry reforming and partial oxidation of methane. *Renew. Energy* **2020**, *149*, 1053–1067. [CrossRef]

31. Alvarez-Galvan, C.; Melian, M.; Ruiz-Matas, L.; Eslava, J.L.; Navarro, R.M.; Ahmadi, M.; Roldan Cuenya, B.; Fierro, J.L.G. Partial Oxidation of Methane to Syngas Over Nickel-Based Catalysts: Influence of Support Type, Addition of Rhodium, and Preparation Method. *Front. Chem.* **2019**, *7*, 104. [CrossRef]

32. Dias, J.A.C.; Assaf, J.M. Influence of calcium content in Ni/CaO/γ-Al$_2$O$_3$ catalysts for CO$_2$-reforming of methane. In Proceedings of the Catalysis Today; Elsevier: Amsterdam, The Netherlands, 2003; Volume 85, pp. 59–68.

33. Claude, V.; Mahy, J.G.; Tilkin, R.G.; Lambert, S.D. Enhancement of the catalytic performances and lifetime of Ni/γ- Al$_2$O$_3$ catalysts for the steam toluene reforming via the combination of dopants: Inspection of Cu, Co, Fe, Mn, and Mo species addition. *Mater. Today Chem.* **2020**, *15*, 100229. [CrossRef]

34. Jing, Z.; Zhang, T.; Shang, J.; Zhai, M.; Yang, H.; Qiao, C.; Ma, X. Influence of Cu and Mo components of γ-Al$_2$O$_3$ supported nickel catalysts on hydrodeoxygenation of fatty acid methyl esters to fuel-like hydrocarbons. *J. Fuel Chem. Technol.* **2018**, *46*, 427–440. [CrossRef]

35. Shah, M.; Bordoloi, A.; Nayak, A.K.; Mondal, P. Effect of Ti/Al ratio on the performance of Ni/TiO$_2$-Al$_2$O$_3$ catalyst for methane reforming with CO$_2$. *Fuel Process. Technol.* **2019**, *192*, 21–35. [CrossRef]

36. Cheng, L.J.; Liu, Z.; Yuan, S.L.; Hu, X.; Zhang, B.; Jiang, Y. Preparation of Ag-Mn/γ-Al$_2$O$_3$-TiO$_2$ catalysts by complexation-impregnation process with citric acid and its application in propane catalytic combustion. *Ranliao Huaxue Xuebao J. Fuel Chem. Technol.* **2019**, *47*, 1379–1385. [CrossRef]

37. Zhang, P.; Mu, F.; Zhou, Y.; Long, Y.; Wei, Q.; Liu, X.; You, Q.; Shan, Y.; Zhou, W. Synthesis of highly ordered TiO$_2$-Al$_2$O$_3$ and catalytic performance of its supported NiMo for HDS of 4, 6-dimethyldibenzothiophene. *Catal. Today* **2020**. [CrossRef]

38. Abdollahifar, M.; Haghighi, M.; Babaluo, A.A.; Talkhoncheh, S.K. Sono-synthesis and characterization of bimetallic Ni-Co/Al$_2$O$_3$-MgO nanocatalyst: Effects of metal content on catalytic properties and activity for hydrogen production via CO$_2$ reforming of CH$_4$. *Ultrason. Sonochem.* **2016**, *31*, 173–183. [CrossRef]

39. Alabi, W.O. CO$_2$ reforming of CH$_4$ on Ni-Al-Ox catalyst using pure and coal gas feeds: Synergetic effect of CoO and MgO in mitigating carbon deposition. *Environ. Pollut.* **2018**, *242*, 1566–1576. [CrossRef]

40. Khoja, A.H.; Tahir, M.; Amin, N.A.S. Cold plasma dielectric barrier discharge reactor for dry reforming of methane over Ni/γ-Al$_2$O$_3$-MgO nanocomposite. *Fuel Process. Technol.* **2018**, *178*, 166–179. [CrossRef]

41. Jang, W.J.; Jung, Y.S.; Shim, J.O.; Roh, H.S.; Yoon, W.L. Preparation of a Ni-MgO-Al$_2$O$_3$ catalyst with high activity and resistance to potassium poisoning during direct internal reforming of methane in molten carbonate fuel cells. *J. Power Sources* **2018**, *378*, 597–602. [CrossRef]

42. Özdemir, H.; Faruk Öksüzömer, M.A. Synthesis of Al$_2$O$_3$, MgO and MgAl$_2$O$_4$ by solution combustion method and investigation of performances in partial oxidation of methane. *Powder Technol.* **2020**, *359*, 107–117. [CrossRef]

43. Xu, L.; Yin, X.L.; Wang, N.; Chen, M. Effect of Y$_2$O$_3$ addition on the densification, microstructure and mechanical properties of MgAl$_2$O$_4$[sbnd]CaAl$_4$O$_7$[sbnd]CaAl$_{12}$O$_{19}$composites. *J. Alloys Compd.* **2017**, *702*, 472–478. [CrossRef]

44. Rittidech, A.; Somrit, R.; Tunkasiri, T. Effect of adding Y$_2$O$_3$ on structural and mechanical properties of Al$_2$O$_3$-ZrO$_2$ ceramics. In Proceedings of the Ceramics International; Elsevier: Amsterdam, The Netherlands, 2013; Volume 39, pp. S433–S436.

45. Santos, D.C.R.M.; Madeira, L.; Passos, F.B. The effect of the addition of Y$_2$O$_3$ to Ni/α-Al$_2$O$_3$ catalysts on the autothermal reforming of methane. *Catal. Today* **2010**, *149*, 401–406. [CrossRef]

46. Ma, H.; Zhang, R.; Huang, S.; Chen, W.; Shi, Q. Ni/Y$_2$O$_3$-Al$_2$O$_3$ catalysts for hydrogen production from steam reforming of ethanol at low temperature. *J. Rare Earths* **2012**, *30*, 683–690. [CrossRef]

47. Sun, L.; Tan, Y.; Zhang, Q.; Xie, H.; Song, F.; Han, Y. Effects of Y$_2$O$_3$-modification to Ni/γ-Al$_2$O$_3$ catalysts on autothermal reforming of methane with CO$_2$ to syngas. *Int. J. Hydrog. Energy* **2013**, *38*, 1892–1900. [CrossRef]

48. Sing, K.S.W.; Everett, D.H.; Haul, R.A.W.; Moscou, L.; Pierotti, R.A.; Rouquerol, J.; Siemieniewska, T. Reporting Physisorption Data for Gas/Solid Systems with Special Reference to the Determination of Surface Area and Porosity. *Pure Appl. Chem.* **1985**, *57*, 603–619. [CrossRef]

49. Li, S.; Gong, J. Strategies for improving the performance and stability of Ni-based catalysts for reforming reactions. *Chem. Soc. Rev.* **2014**, *43*, 7245–7256. [CrossRef]

50. Costa, D.S.; Gomes, R.S.; Rodella, C.B.; da Silva, R.B.; Fréty, R.; Teixeira Neto, É.; Brandão, S.T. Study of nickel, lanthanum and niobium-based catalysts applied in the partial oxidation of methane. *Catal. Today* **2020**, *344*, 15–23. [CrossRef]

51. Cheephat, C.; Daorattanachai, P.; Devahastin, S.; Laosiripojana, N. Partial oxidation of methane over monometallic and bimetallic Ni-, Rh-, Re-based catalysts: Effects of Re addition, co-fed reactants and catalyst support. *Appl. Catal. A Gen.* **2018**, *563*, 1–8. [CrossRef]

Sample Availability: Structure of the compounds and trajectories are available from the authors.